OFFICE OF NAVAL RESEARCH

CONTRACT N00014-84-K-0274

Task No. NR 039-260

TECHNICAL REPORT NO. 3

WLF Dependence of the Dielectric Properties of DGEBA Epoxy Resins

by

Norman F. Sheppard, Jr. and Stephen D. Senturia

Submitted for Publication

in

Journal of Polymer Science, Polymer Physics Ed.

MASSACHUSETTS INSTITUTE OF TECHNOLOGY

Department of Electrical Engineering and Computer Science

Cambridge, Massachusetts

August 23, 1985

SECURITY CLASSIFICATION OF THIS PAGE (When Data Entered)

REPORT DOCUMENTATION PAGE		READ INSTRUCTIONS BEFORE COMPLETING FORM
1. REPORT NUMBER	2. GOVT ACCESSION NO. AD-A159 224	3. RECIPIENT'S CATALOG NUMBER
4. TITLE (and Subtitle) WLF Dependence of the Dielectric Properties of DGEBA Epoxy Resins		5. TYPE OF REPORT & PERIOD COVERED Technical Report 5/1/84-8/31/85
		6. PERFORMING ORG. REPORT NUMBER Technical Report No. 3
7. AUTHOR(s) Norman F. Sheppard, Jr. and Stephen D. Senturia		8. CONTRACT OR GRANT NUMBER(s) N00014-84-K-0274
9. PERFORMING ORGANIZATION NAME AND ADDRESS Massachusetts Institute of Technology 77 Massachusetts Avenue Cambridge, MA 02139		10. PROGRAM ELEMENT, PROJECT, TASK AREA & WORK UNIT NUMBERS NR 039-260
11. CONTROLLING OFFICE NAME AND ADDRESS Department of the Navy, Office of Naval Research 800 N. Quincy Street Arlington, VA 22217		12. REPORT DATE 8/23/85
		13. NUMBER OF PAGES 29
14. MONITORING AGENCY NAME & ADDRESS(if different from Controlling Office)		15. SECURITY CLASS. (of this report) UNCLASSIFIED
		15a. DECLASSIFICATION/DOWNGRADING SCHEDULE

16. DISTRIBUTION STATEMENT (of this Report)

This document has been approved for public release and sale; its distribution is unlimited.

17. DISTRIBUTION STATEMENT (of the abstract entered in Block 20, if different from Report)

18. SUPPLEMENTARY NOTES

19. KEY WORDS (Continue on reverse side if necessary and identify by block number)

Williams-Landel-Ferry equation, WLF equation, dielectric properties, DGEBA epoxy resins, ionic conductivity, dipole relaxation, microdielectrometry

20. ABSTRACT (Continue on reverse side if necessary and identify by block number)

The frequency and temperature dependence of the complex dielectric constant (ϵ^*) of seven diglycidyl ether of bisphenol-A (DGEBA) epoxy resins having epoxide equivalent weights (EEW) in the range 175 to 1880 have been measured from T_g-30 C to T_g+70 C at frequencies between 0.1 and 10,000 Hz. In the vicinity of T_g, ϵ^* is dominated by dipole relaxation, while at higher temperatures ionic conductivity dominates. For all resins, the temperature dependences of the frequency of maximum

DD FORM 1 JAN 73 1473 EDITION OF 1 NOV 65 IS OBSOLETE
S/N 0102-014-6601

SECURITY CLASSIFICATION OF THIS PAGE (When Data Entered)

dipole loss, f_{max}, and of the conductivity, σ, obey the Williams-Landel-Ferry (WLF) equation. The WLF constants C_1 and C_2 were determined for both the f_{max} and σ data for each of the resins. In a given material, the WLF constants for σ and f_{max} differed, indicating that the temperature dependences of the mobilities of ionic impurities and permanent dipole moments differ quantitatively. As the EEW of the material increased, the C_1 constants for the conductivity remained constant, while the C_2 constants increased. The C_1 constants for f_{max} decreased with increasing resin EEW, approaching the C_1 values determined for the conductivity at high EEW's, while the corresponding C_2 constants decreased slightly. Free volume and entropic theories of the glass transition are used to interpret these results in terms of the underlying conduction and dipole relaxation processes.

WLF Dependence of the Dielectric Properties of DGEBA Epoxy Resins

Norman F. Sheppard, Jr. and Stephen D. Senturia
Massachusetts Institute of Technology
Cambridge, Massachusetts

Synopsis

The frequency and temperature dependence of the complex dielectric constant (ε^*) of seven diglycidyl ether of bisphenol-A (DGEBA) epoxy resins having epoxide equivalent weights (EEW) in the range 175 to 1880 have been measured from T_g-30°C to T_g+70°C at frequencies between 0.1 and 10,000 Hz. In the vicinity of T_g, ε^* is dominated by dipole relaxation, while at higher temperatures ionic conductivity dominates. For all resins, the temperature dependences of the frequency of maximum dipole loss, f_{max}, and of the conductivity, σ, obey the Williams-Landel-Ferry (WLF) equation. The WLF constants C_1 and C_2 were determined for both the f_{max} and σ data for each of the resins. In a given material, the WLF constants for σ and f_{max} differed, indicating that the temperature dependences of the mobilities of ionic impurities and permanent dipole moments differ quantitatively. As the EEW of the material increased, the C_1 constants for the conductivity remained constant, while the C_2 constants increased. The C_1 constants for f_{max} decreased with increasing resin EEW, approaching the C_1 values determined for the conductivity at high EEW's, while the corresponding C_2 constants decreased slightly. Free volume and entropic theories of the glass transition are used to interpret these results in terms of the underlying conduction and dipole relaxation processes.

INTRODUCTION

The measurement of dielectric properties is widely used as a means of studying the cure of of thermosetting polymers because it is one of the few methods that can follow the complete transformation from liquid resin to glassy solid. The dielectric properties of these materials depend on the mobilities of ionic impurities and of permanent dipole moments, both of which decrease by many orders of magnitude during cure. There is evidence in the literature of a correlation between viscosity and both mean dipole relaxation time [1,2] and ionic conductivity [3,4]. Recent studies of thermosets [5,6,7] have attempted to model the temperature and cure dependence of the viscosity using a Williams-Landel-Ferry (WLF) equation [8], but modified to include the dependence of the glass transition temperature, T_g, on chemical conversion. While there is considerable evidence that the temperature dependence of the mean dipole relaxation time [9] and ionic conductivity [10-13] in polymers can be modeled using the WLF equation, this approach has not yet been used to model the dielectric properties during cure. However, given the relationship between the dielectric properties and the viscosity, such modeling should be successful.

The purpose of this work is to make a first step in the WLF modeling of dielectric properties of curing epoxy systems. The WLF approach would require measuring the temperature dependence of the quantity of interest at fixed chemical conversion. This paper reports a simpler study of the dielectric properties of a homologous series of DGEBA epoxy resins of varying molecular weights (without curing agent). The insights drawn from this study about the application of the WLF equation

to the dielectric properties during cure will be discussed in the conclusion.

EXPERIMENTAL

The epoxy resins used were seven commercial samples of diglycidyl ether of bisphenol-A (DGEBA) resins having epoxide equivalent weights ranging from 175 to 1880. The structural formula of DGEBA is illustrated in Figure 1. Table 1 presents epoxide equivalent weight, the n value calculated from the EEW, and the T_g measured at 10°C/min using DSC. Prior to use, the samples were heated under vacuum to remove water and other volatiles.

The dielectric measurements were performed using microdielectrometry [14,15], which utilizes a silicon integrated circuit sensor having a comb electrode pattern, amplifying circuitry, and a semiconductor diode for temperature measurement. The sample to be measured is placed on the surface of the sensor, in intimate contact with the comb electrode pattern. Utilizing additional amplifying circuitry and a Fourier transform signal source/correlator, the electrical admittance of the comb electrode pattern can be measured at frequencies ranging from 0.005 Hz to 10,000 Hz. The calibration of the sensor in terms of the complex permittivity is based on a numerical solution to Laplace's equation [16]. The maximum electric field is approximately 1000 V/cm.

The electrode area of the microdielectrometry sensor is 2 x 3.5 mm. Resin samples of less than 10 mg were applied to the sensors by heating the sensor on a hot plate and melting the resin over the comb electrode structure. The sensor was placed into a programmable sample chamber

under nitrogen and the room temperature reading of the diode temperature indicator was calibrated against a thermocouple embedded in the sensor holder. The sample was then cooled or heated to the starting temperature and the temperature program and data acquisition, under computer control, was initiated. The temperature was increased from approximately T_g - 30°C to T_g + 70°C in discrete steps of 4°C. At each temperature, the dielectric permittivity and loss factor were measured at 26 frequencies in the range of 0.1 to 10,000 Hz.

RESULTS AND DISCUSSION

Conductivity and Frequency of Maximum Dipole Loss

Figure 2 illustrates the temperature dependence of the dielectric permittivity and loss factor for EPON 828 resin, which has a glass transition temperature of -17°C. At temperatures well below T_g, the permittivity at all frequencies has a value of 4.2, and the loss factor is below 0.1. As the temperature approaches T_g, the dipoles gain sufficient mobility to orient partially during one cycle of the alternating field. The permittivity and loss factor at the lowest frequencies begin to increase first. With a further increase in temperature, the permittivity for a given frequency levels off, starts to decrease (a thermal effect [17,18]), and then abruptly increases again as a result of electrode polarization [19]. A dipole loss peak is observed in the loss factor, which then rises continuously with temperature due to an increasing ionic conductivity. The frequency at which the dipole loss peak occurs is proportional to the average dipole mobility. The ionic conductivity is proportional to the mobility of ionic impurities, pro-

vided the ion concentration remains fixed. This is a reasonable assumption since the ionic species are predominantly sodium and chloride remaining from the synthesis procedure [20,21], although there has been no explicit verification for the specific epoxy samples reported on here. Both the frequency of maximum loss, f_{max}, and the ionic conductivity increase by many orders of magnitude over a narrow temperature range, a characteristic of relaxation processes very close to the glass transition temperature.

The frequency dependence of the loss factor at fixed temperature, shown for three different temperatures in Figure 3, illustrates the mechanisms of ionic conductivity and dipole relaxation. At the highest temperature, 22°C, the loss factor is inversely proportional to frequency, with a slope on a log-log plot very near to -1. This behavior is characteristic of a frequency independent ionic conductivity, σ, which is related to the loss factor by the equation,

$$\sigma = \varepsilon'' \varepsilon_0 \omega \qquad (1)$$

where ε_0 is the permittivity of free space and ω is the angular frequency. If electrode polarization effects were present in the loss factor data, the slope would decrease as the frequency decreased. Conductivity results presented here are taken from loss factor data where polarization effects are absent.

At the lowest temperature, -12°C, there is a peak in the loss factor having a maximum value of about 2, characteristic of a dipole relaxation process. The asymetric shape of this peak is well described by a Williams-Watts function [22]. This will be discussed in more detail in a separate communication. The present analysis is concerned

only with the average dipole mobility, characterized by the frequency of maximum loss. At an intermediate temperature, 5°C, the ionic conductivity is observed at low frequencies, while the onset of the dipole loss peak is seen at high frequencies.

The temperature dependent conductivities of all of the resin samples, determined at frequencies where the loss factor is inversely proportional to frequency, are shown plotted in Arrhenius fashion in Figure 4. There is significant curvature in this plot, indicating that the conduction process is not simply activated, and suggesting a process described by the WLF equation. The solid curves through the data points represent the fit to the WLF equation, to be discussed below.

The temperature dependence of the frequency of maximum loss for each resin sample was determined directly from the loss factor versus temperature data by identifying the dipole loss peak temperature for each frequency. An Arrhenius plot of the f_{max} data is presented in Figure 5. Although not as pronounced as the conductivity data, careful examination of the data reveals curvature characteristic of WLF rather than Arrhenius behavior. The smaller curvature is due to the fact that the dipole relaxation occurs at temperatures much closer to the glass transition and over a much narrower temperature range. The apparent activation energies calculated from the data are in the range 350-500 kJ/mol, extremely large for a thermally activated process. The solid curves represent the fit to the WLF equation, to be described below.

Williams-Landel-Ferry Equation

The Williams-Landel-Ferry (WLF) equation [8] is expressed as,

$$\log (a_T) = \frac{- C_1 (T - T_s)}{C_2 + T - T_s} \qquad (2)$$

where a_T is the shift factor, originally defined as the ratio of the viscosity at temperature T to that at a reference temperature, T_s. C_1 and C_2 are constants which depend on the reference temperature chosen and on the material. The constants were originally thought to be universal, having values of 17.44 and 51.6 when the reference temperature was taken as the dilatometric glass transition temperature. The universality of this equation was attributed to relaxation processes governed by free volume. By combining Doolittle's free volume theory of viscosity [23] with a free volume that increases linearly with temperature above the glass transition temperature, the constants C_1 and C_2 can be expressed in terms of f_g, the free volume fraction of the glass, and a free volume thermal expansion coefficient, $\Delta\alpha$, taken to be the difference in the thermal expansion coefficients above and below the glass transition temperature.

$$C_1 = \frac{1}{2.3\ f_g} \qquad C_2 = \frac{f_g}{\Delta\alpha} \qquad (3)$$

The proposal by Fox and Flory [24] that T_g is an iso-free-volume state (f_g constant) and experimental evidence [8] showing that $\Delta\alpha$ is approximately constant for a large number of polymers supported the argument that the WLF constants were universal.

To explain the subsequent observation that the constants C_1 and C_2 were not universal, Cohen and Turnbull [25] proposed a theory for transport based on free volume in which a critical free volume, V^*, resulting from redistribution of free volume without a change in energy, is required for a particle to diffuse. This theory leads to the WLF equation, with the constants equal to [10],

$$C_1 = \frac{\gamma f^*}{2.3\ f_g} \qquad C_2 = \frac{f_g}{\Delta\alpha} \qquad (4)$$

where γ is a factor to account for the overlap of free volume [25], and f^* is the critical free volume fraction. Since the critical free volume will depend on the particle or molecule diffusing, this theory helps account for the observed material dependence of the constants. When the theory is applied to dielectric relaxation of polymers, the critical free volume is interpreted as that volume necessary for the polar segment to relax. In recent work in which the ionic conductivity of polymers was interpreted in terms of WLF theory [10,11], the critical free volume has been interpreted as that volume required for ion transport.

Adam and Gibbs [26] proposed a theory for cooperative relaxation processes in polymers near T_g based on Gibbs and Dimarzio's entropic theory for the glass transition [27]. The theory assumes a configurational entropy which goes to zero at a temperature T_2. A second order phase transition would occur at T_2 if the rate of molecular rearrangement, which depends on the configurational entropy, did not become infinitesimal. The glass transition is observed experimentally at a

temperature $T_g > T_2$, which is the temperature at which the time scale for molecular rearrangement becomes comparable to the time scale of the experiment.

The Adam and Gibbs theory relates the relaxational properties of polymers to the Gibbs and Dimarzio second order transition temperature, T_2. The basis of the theory is that the number of segments required for a cooperative relaxation increases as the temperature decreases, making the relaxation process more difficult. An average transition probability, W(T), is derived,

$$W(T) = A \exp(-z^* \Delta\mu / kT) \qquad (5)$$

where z^* is the number of molecules or segments involved in the relaxation, and $\Delta\mu$ is the free energy barrier per molecule or segment. Assuming the cooperatively rearranging regions to be noninteracting subsystems, z^* is expressed in terms of s_c^*, a critical entropy for rearrangement, and the configurational entropy per segment, equal to the molar configurational entropy of the sample, S_c, divided by Avogadro's number, N_{av}.

$$z^* = N_{av} s_c^* / S_c \qquad (6)$$

As the temperature is lowered and the molar configurational entropy, S_c, approaches zero, z^* gets very large, and the average transition probability W(T) gets very small. The temperature dependence of the entropy term S_c is expressed in terms of the change in specific heat at the glass transition, ΔC_p,

$$S_c(T) = \Delta C_p \ln (T / T_2) \qquad (7)$$

recalling that the configurational entropy is zero at temperature T_2. Note that this equation does not include any ionic contribution to the entropy; nor are the ions presumed to participate in the initial partitioning of the system into segments in Eq. 6. This point will be addressed later as possibly affecting the difference between the f_{max} and conductivity C_2 constants.

The shift factor, a_T, can be expressed as a ratio of transition probabilities at temperatures T and T_s, and rearranged to yield an expression in the form of the WLF equation,

$$\log (a_T) = \log (W(T_s) / W(T)) = \frac{- C_1 (T - T_s)}{C_2 + (T - T_s)} \qquad (8)$$

where the WLF constants C_1 and C_2 are approximately,

$$C_1 = \frac{2.303 s_c^* \Delta\mu}{k \Delta C_p T_s \ln (T_s / T_2)} \qquad C_2 = \frac{T_s \ln (T_s / T_2)}{1 + \ln (T_s / T_2)} \qquad (9)$$

The WLF constants can be expressed in terms of the "true" second order transition temperature T_2, and the energy barrier $\Delta\mu$. Adam and Gibbs found "universal" values of $T_g/T_2 = 1.3$ and $T_g - T_2 = 55^\circ C$, and estimated $\Delta\mu$ to be comparable to molecular interaction energies [26].

Interpretation of C_1 and C_2

The results presented in the Arrhenius plots of Figures 4 and 5 suggested that both the conductivity and the frequency of maximum loss

could be represented by the WLF equation. The substitution of σ or f_{max} for viscosity in the definition of the shift factor, a_T, necessitated a sign change in Equation 2, because both σ and f_{max} increase with increasing temperature. To determine C_1 and C_2 for a given material, a variation of the standard WLF test plot procedure [8], shown in Figure 6, was used. Each of the data points was used as a trial reference temperature, and the resulting values of C_1 and C_2 were then normalized to a reference temperature equal to the glass transition temperature determined from the DSC. The set of normalized constants, which agreed to ±10% for the conductivity data and ±20% for the f_{max} data, were then averaged to obtain the "best fit" C_1 and C_2 values for that material. These values are presented in Table 2 for the conductivity and in Table 3 for the frequency of maximum loss. The constants in the Tables were used to draw the solid curves through the data in Figures 4 and 5.

The conductivity C_1 constant is independent of the EEW of the resin, while the f_{max} C_1 constant and the C_2 constants are EEW dependent. For the cases that are EEW dependent, note that the values for the two low molecular weight resins are similar to one another, as are those for the four high EEW resins, while the n=0.6 resin values are intermediate. The conductivity at T_g increases with increasing EEW of the resin, while $f_{max}(T_g)$ is approximately constant. The variation in $\sigma(T_g)$ for the different resins is too large to attribute to variations in ionic impurity concentration and, instead, is attributable to a basic difference between ion mobility and polymer chain mobility. This is discussed in detail below. The approximately constant value of $f_{max}(T_g)$ indicates a correlation between the DSC glass transition temperature and

the dipole loss peak measured at a frequency of approximately 3 Hz. A similar correlation between the low frequency dipole loss peak and vitrification has been observed in curing systems [18].

Assuming that T_g is an iso-free-volume state (f_g constant) [24], and the overlap factor γ is independent of EEW, Cohen and Turnbull's model described above predicts that the C_1 constants for conductivity and f_{max} are proportional to critical volumes for ion transport, V_i^*, and for polar segmental motion, V_s^*, respectively. The C_1 behavior indicates that the critical volume for ion transport, V_i^*, is independent of EEW. This is not surprising because of the small size of the ionic impurities relative to the resin molecules; even the lowest EEW resin is large compared to the ion. The observed decrease in V_s^*, the critical volume for segmental motion, suggests the volume required to relax a typical dipolar segment decreases with increasing EEW. This result may not be due to the increased chain length, but to the changing chemical composition. Referring back to Figure 1, two types of polar segments can be identified: a glycidyl ether unit at the chain end and a hydroxyether segment in the backbone of the oligomers. As the molecular weight of the resin increases, there is a systematic increase in the fraction of hydroxyether segments. Assuming all of the DGEBA resins are linear molecules, and the polarities of the two types of segments are approximately the same, the fraction of hydroxyether segments in a sample of given EEW will be equal to $n/(2+n)$. If the critical volume for segmental relaxation can be expressed in terms of a number average of that for a hydroxyether segment (HE) and of a glycidyl ether segment (GE), then C_1 can be expressed as,

$$C_1 = \frac{2}{(2+n)} C_{1,GE} + \frac{n}{(2+n)} C_{1,HE} \qquad (10)$$

This n-dependence can be illustrated as follows. Taking $C_{1,HE}$ as equal to 10.5, the average value obtained from the ionic conductivity analysis, and taking $C_{1,GE}$ as twice $C_{1,HE}$ yields the solid line plotted in Figure 7. The agreement is qualitative at best, but supports the hypothesis that the C_1 value is related to the type of polar segment relaxing. A possible explanation for the difference in critical relaxation volumes for the two segments is that the hydroxyether may relax by a crankshaft mechanism with minimal involvement of neighboring molecules, whereas the relaxation of the glycidyl ether requires cooperative motion of neighboring molecules.

The free volume theory is unable to explain the behavior of the C_2 constants. Referring back to Equation 2, the C_2 constant depends only on f_g, the free volume fraction at T_g, and $\Delta\alpha$, the difference in thermal expansion coefficients above and below T_g. On this basis, the C_2 values should be the same for the f_{max} and the conductivity data, but the C_2 values determined from the conductivity data increase with increasing EEW, while those determined from the f_{max} data decrease slightly.

The Adam-Gibbs thermodynamic theory provides an expression for C_2 in terms of the second order transition temperature, T_2, which can be determined directly from C_2 using Equation 8. The results of this analysis for the f_{max} data are presented in Table 4. The T_2 values range from 175 K for the n=0.2 sample to 309 K for the n=12.1 sample, while the corresponding values of T_g are 257 K and 352 K, respectively. The average value of T_g-T_2 for the seven samples is 60°C ± 21% which is

consistent with the value of 55° ± 11% found by Adam and Gibbs for a wide variety of polymers [26]. The same analysis was repeated for the conductivity data and the results are presented in Table 5. The T_2 values range from a low of 209 K for the n=2.3 sample to 259 K for the n=12.1 sample. These values are significantly different than those determined from the f_{max} data. This is emphasized in Figure 8, which is a plot of the T_2 values versus the T_g of the resins. The f_{max} values scatter about a line with a slope of 1.2, while the conductivity T_2 values are relatively independent of T_g.

The correlation of the T_2's from the f_{max} data with T_g indicates that the temperature dependence of the configurational entropy function governing the heat capacity change at T_g measured by the DSC is similar to that governing the dipole relaxation. The constant values of f_{max} at the DSC T_g are a manifestation of this. The relative insensitivity of the conductivity T_2 values to T_g indicates that cooperative molecular relaxation processes are only a part of the conduction process. The wide variation in $\sigma(T_g)$ for the different resins is consistent with this interpretation. The application of the Adam-Gibbs theory to the ionic conductivity may require a reformulation or redefinition of the critical segment (Eq. 6) and/or the relevant configuration entropy term (Eq. 7), to account for the additional configurational states available to ions. Such a reformulation has not been carried out.

CONCLUSION

The temperature dependences of the conductivity and frequency of maximum loss in DGEBA epoxy resins near T_g are described by different

WLF equations, due to the differing natures of the conduction and dipole relaxation processes. The WLF C_1 constants reflect critical volumes for ion transport and dipolar segment motion. The critical volumes for ion transport are independent of resin EEW, because of the small size of ionic impurities relative to the resin molecules. The EEW dependence of the critical volumes for polar segmental motion correlates with the relative concentrations of glycidyl ether and hydroxyether segments, leading to speculation that the hydroxyether relaxes by a crankshaft mechanism with miminal involvement of neighboring molecules, while the glycidyl ether requires cooperative motion of neighbors.

The Adam-Gibbs entropic theory of the glass transition was used to determine the Gibbs-Dimarzio second order transition temperatures, T_2, from the WLF C_2 constants. For the f_{max} data, T_2 values were about 60° below T_g. The T_2 values determined from the conductivity data were relatively independent of T_g, indicating that degrees of freedom in addition to the polymer chain configurations are required for the ionic conduction process, and that proper application of this theory to conduction will require reformulation to account for these additional degrees of freedom.

An important conclusion to be drawn from these results is that to first order, the parameters C_1 and T_2 describing the temperature dependence of the conductivity are both relatively independent of the detailed chemical structure of the sample. Therefore, in curing systems, if the constancy of C_1 and T_2 can be assumed, it should be possible to follow the change in T_g during cure using the measured conductivity

change and the WLF equation. Results supporting this idea will be presented in a separate communication.

ACKNOWLEDGEMENT

This work was supported in part by the Office of Naval Research. The authors wish to thank James Lemay of the University of Akron and William Varnell of Shell Development Company for supplying some of the samples used in this study.

REFERENCES

1. C. Huraux and A. Soualmia, C.R. Acad. Sci. Paris, Serie B, 277, 497 (1973)

2. J.W. Lane, M.A. Bachmann and J.C. Seferis, Proc. 43rd SPE ANTEC, Washington, D.C., April 1985, p. 318.

3. W.E. Baumgartner and T. Ricker, SAMPE J., 19(4), 6 (1983)

4. R.J. Armstrong, Solid State Technology, p. 50, Nov. 1969.

5. Y.A. Tajima and D.G. Crozier, Polym. Eng. Sci., 23, 186 (1983)

6. T.H. Hou, Proc. 43rd SPE ANTEC, Washington, D.C., April 1985, p. 1253.

7. L. Nicolais, "Characterization for Quality Control in Thermosetting Based Composites", 43rd SPE ANTEC, Washington, D.C., April 1985; and private communication.

8. M.L. Williams, R.F. Landel and J.D. Ferry, J. Am. Chem. Soc., 77, 3701 (1955)

9. N.G. McCrum, B.E. Read and G. Williams, Anelastic and Dielectric Effects in Polymeric Solids, Wiley, New York, 1967

10. A. Killis, J-F. LeNest, H. Cheradame and A. Gandini, Makromol. Chem., 183, 2835 (1982)

11. T. Miyamoto and K. Shibayama, J. Appl. Phys., 44, 12 (1973)

12. H. Cheradame, IUPAC Macromolecules, Ed. by H. Benoit and P. Rempp, Pergamon Press, Oxford and New York, 1982.

13. K.Arai and A.Eisenberg, J. Macromol. Sci.-Phys., B17(4), 803 (1980)

14. N.F. Sheppard, S.L. Garverick, D.R. Day and S.D. Senturia, Proc. 26th SAMPE Symposium, Los Angeles, April 1981, p. 65.

15. N.F. Sheppard, D.R. Day, H.L. Lee and S.D. Senturia, Sensors and Actuators, 2, 263 (1982)

16. H.L. Lee, E.E. Thesis, Massachusetts Institute of Technology, 1983, unpublished.

17. N.F. Sheppard and S.D. Senturia, Abstracts 8th Annual Adhesion Society Meeting, Savannah, Georgia, February 1985.

18. N.F. Sheppard, M.C.W. Coln and S.D. Senturia, Proc. 29th SAMPE Symposium, Reno, April 1984, p. 1243.

19. D.R. Day, T.J. Lewis, H.L. Lee and S.D. Senturia, J. Adhesion, 18, 73 (1985)

20. H. Lee and K. Neville, Handbook of Epoxy Resins, McGraw-Hill, New York, 1967.

21. G.L. Hagnauer, AMMRC TR 79-59, Army Materials and Mechanics Research Center, Watertown, Massachusetts, 1979.

22. G. Williams and D.C. Watts, Trans. Farad. Soc., 66, 80 (1970)

23. A.K. Doolittle, J. Appl. Phys., 22, 1471 (1951)

24. T.G. Fox and P.J. Flory, J. Appl. Phys., 21, 581 (1950)

25. M.H. Cohen and D. Turnbull, J. Chem. Phys., 31, 1164 (1959)

26. G. Adam and J.H. Gibbs, J. Chem. Phys., 43, 139 (1965)

27. J.H. Gibbs and E.A. Dimarzio, J. Chem. Phys., 28, 373 (1958)

Table 1 - Epoxy Resin Samples

Sample	EEW	n	Tg(°C)
EPON X22	175[1]	0	-19
EPON 828	185[1]	0.1	-17
EPON 834	255[1]	0.6	-4
EPON 1001F	490[2]	2.3	42
EPON 1002F	660[2]	3.4	51
EPON 1004F	900[2]	5.1	61
EPON 1007F	1880[2]	12.1	79

[1] Values from [20]

[2] Samples and EEW's by titration supplied by J. LeMay, Univ. of Akron

EPON is a registered trademark of Shell Chemical Co.

Table 2 - WLF Constants for σ

ID	n	C_1	C_2(°C)	$\log[\sigma(T_g)]$
X22	0	10.2 ± 0.1	34 ± 3	-15.7
828	0.2	10.3 ± 0.1	30 ± 5	-16.1
834	0.6	10.1 ± 0.2	49 ± 6	-15.4
1001	2.3	11.5 ± 0.6	92 ± 10	-14.1
1002	3.4	10.1 ± 0.2	71 ± 5	-14.7
1004	5.1	11.3 ± 0.4	82 ± 9	-15.3
1007	12.1	10.3 ± 0.4	83 ± 11	-14.5

Table 3 - WLF Constants for f_{max}

ID	n	C_1	C_2(°C)	$\log[f_{max}(T_g)]$
X22	0	21.4 ± 3.5	61 ± 12	-0.1
828	0.2	21.2 ± 3.5	71 ± 13	0.3
834	0.6	15.2 ± 2.7	48 ± 10	-0.2
1001	2.3	12.5 ± 1.0	51 ± 4	1.3
1002	3.4	12.7 ± 1.8	53 ± 8	0.8
1004	5.1	13.4 ± 1.4	55 ± 7	0.5
1007	12.1	11.6 ± 1.2	40 ± 6	0.1

Table 4 - Adam-Gibbs Analysis for f_{max} data

n	C_2	T_g	T_2	T_g-T_2
0	61	254	185	69
0.2	71	257	175	82
0.6	47	269	217	52
2.3	51	315	259	56
3.4	52	324	267	57
5.1	55	334	274	60
12.1	40	352	309	43

Table 5 - Adam-Gibbs Analysis for conductivity data

n	C_2	T_g	T_2	T_g-T_2
0	34	254	217	37
0.2	29	257	225	32
0.6	48	269	215	54
2.3	91	315	209	106
3.4	71	324	245	79
5.1	81	334	242	92
12.1	82	352	259	93

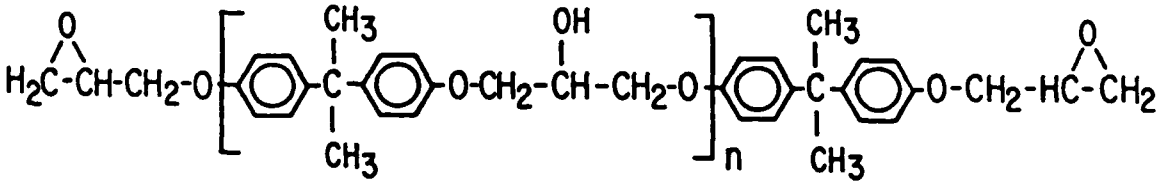

1. Structure of diglycidyl ether of bisphenol-A (DGEBA)

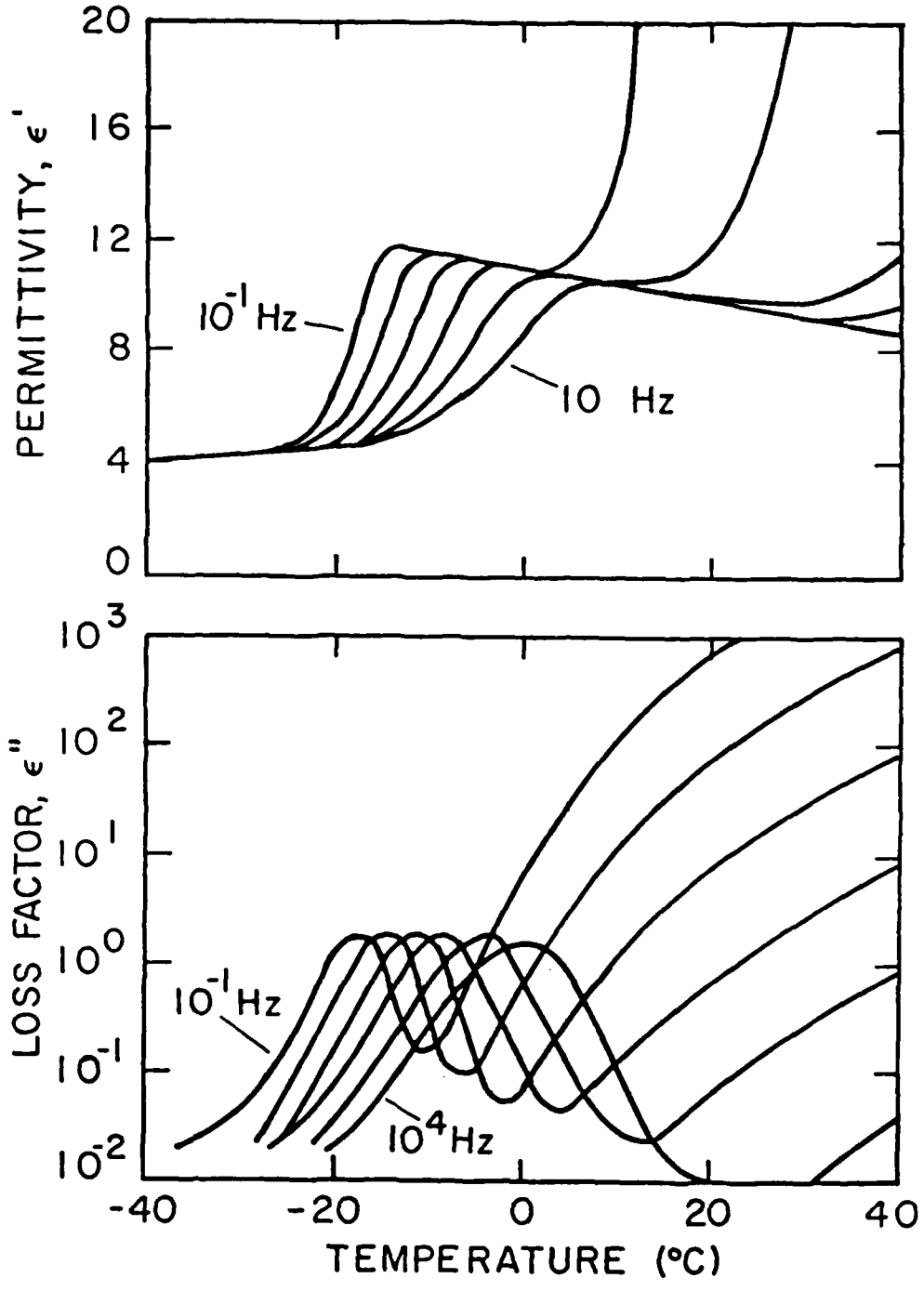

2. Permittivity, ε', and loss factor, ε", versus temperature for EPON 828 at frequencies of 0.1, 1, 10, 100, 1000 and 10,000 Hz.

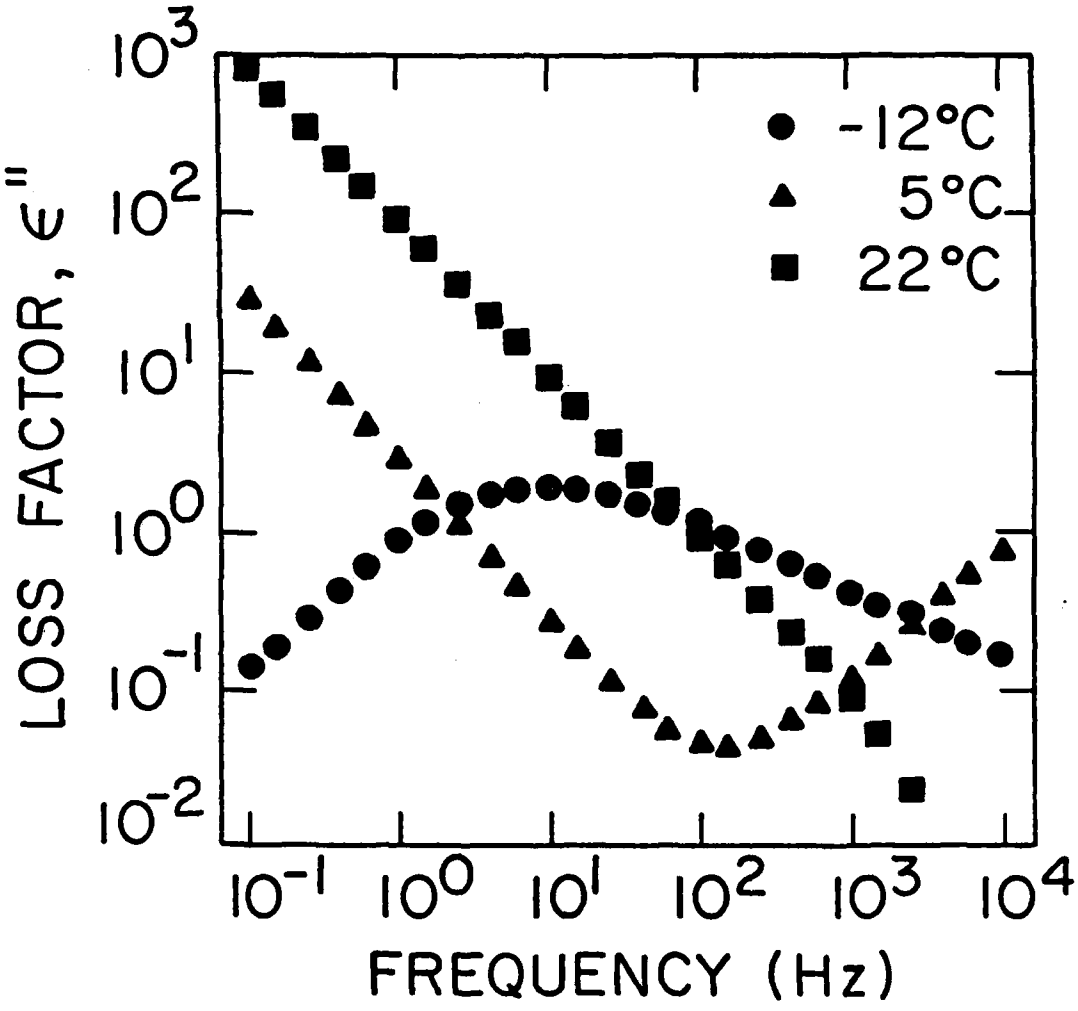

3. Loss factor, ε", versus frequency for EPON 828 at temperatures of -12°C, 5°C and 22°C.

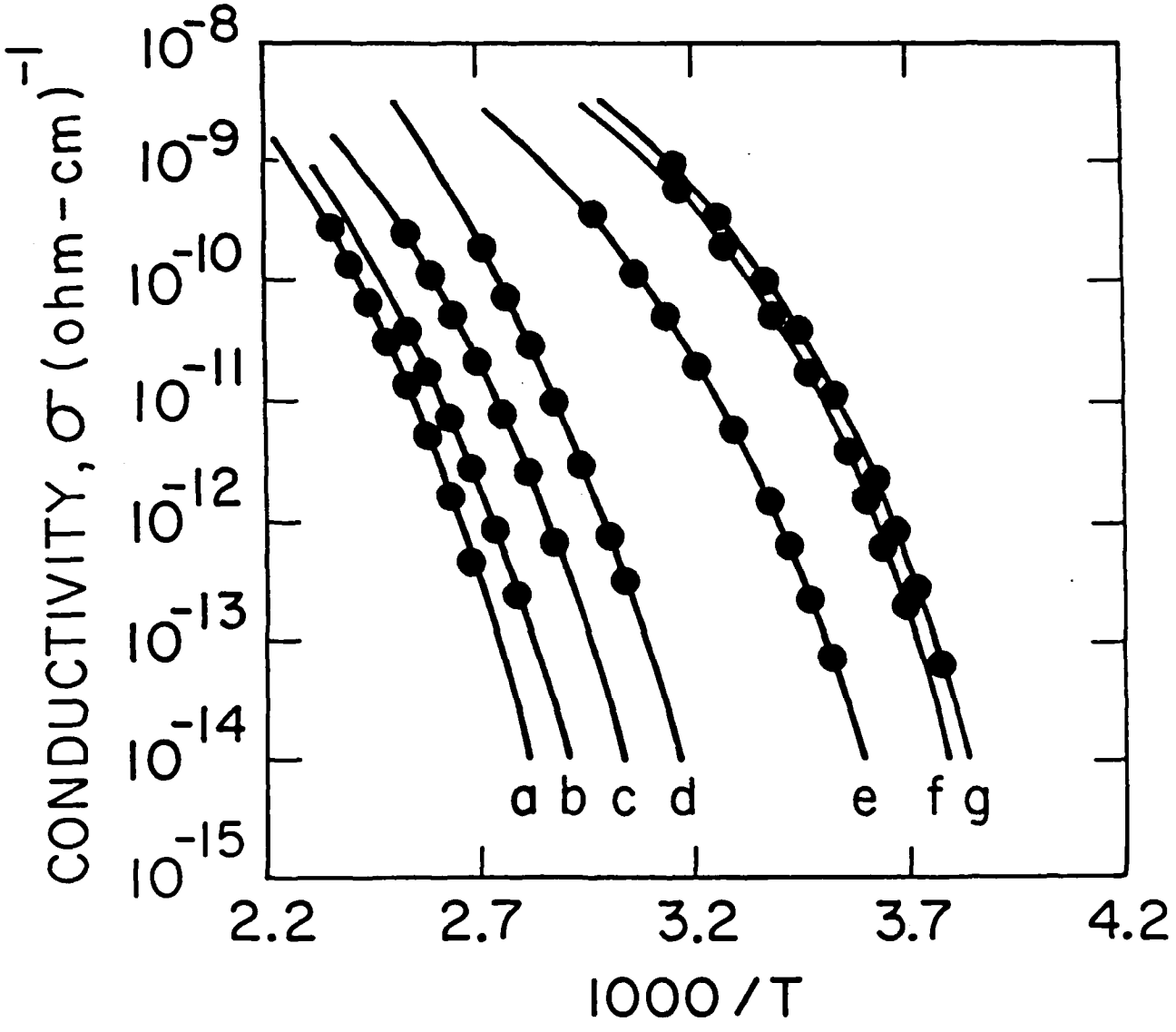

4. Arrhenius plot of ionic conductivity, σ, of EPON resins.
a - 1007, b - 1004, c - 1002, d - 1001, e - 834, f - 828, g - X22

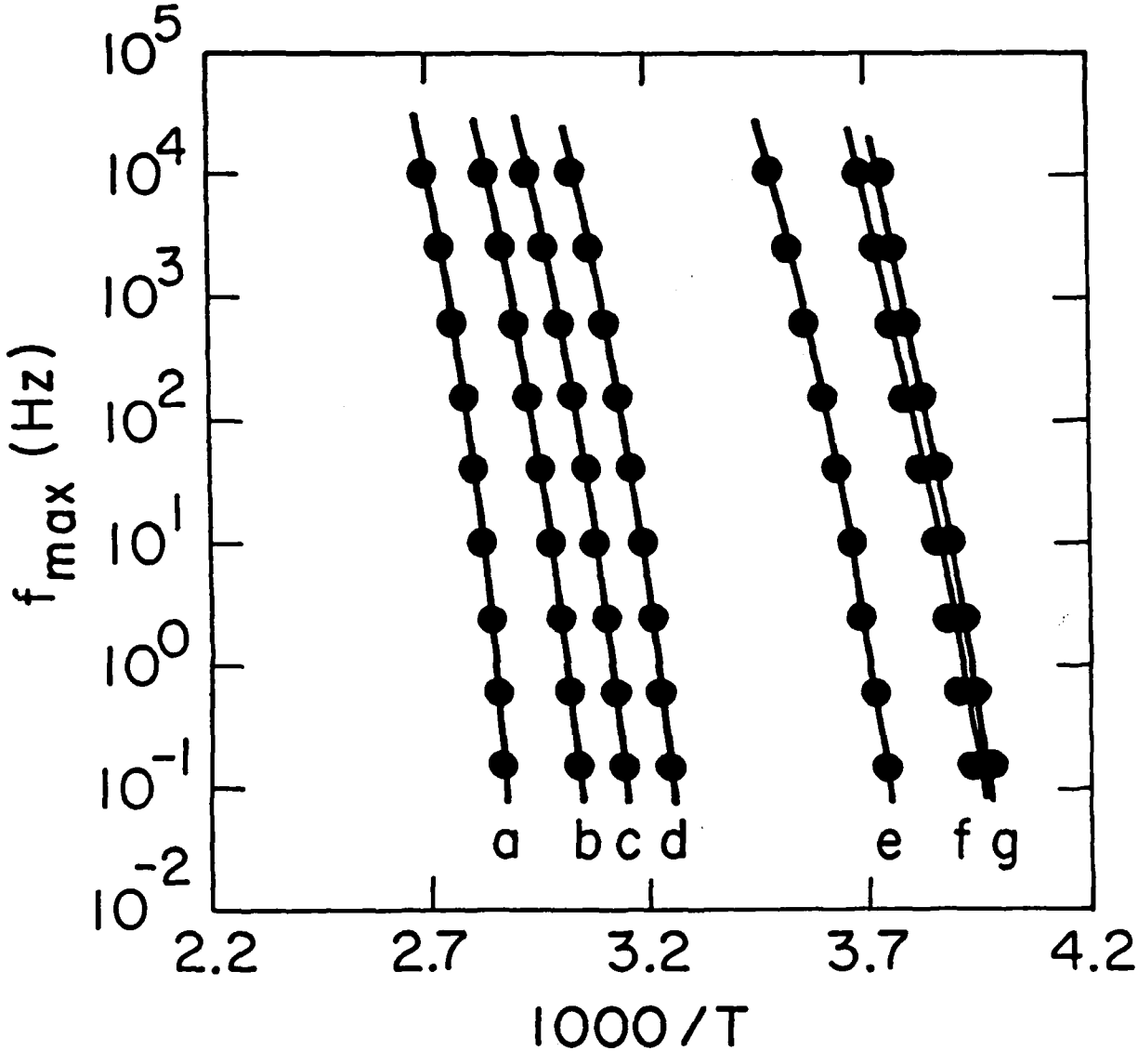

5. Arrhenius plot of frequency of maximum dipole loss, f_{max}, of EPON resins.
a - 1007, b - 1004, c - 1002, d - 1001, e - 834, f - 828, g - X22

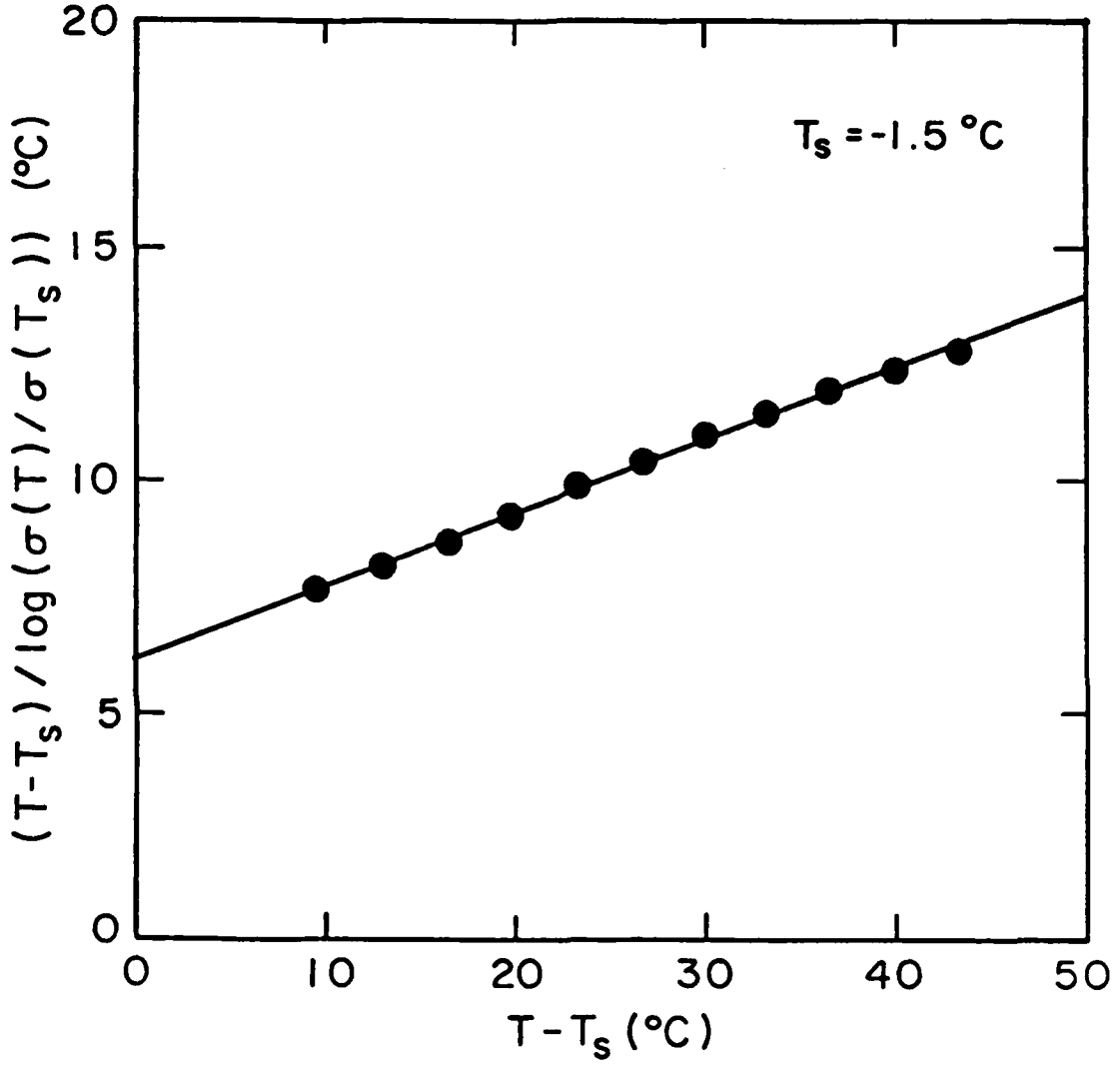

6. Test plot of Williams-Landel-Ferry equation for EPON 828 ionic conductivity data, using a reference temperature of -1.5°C.

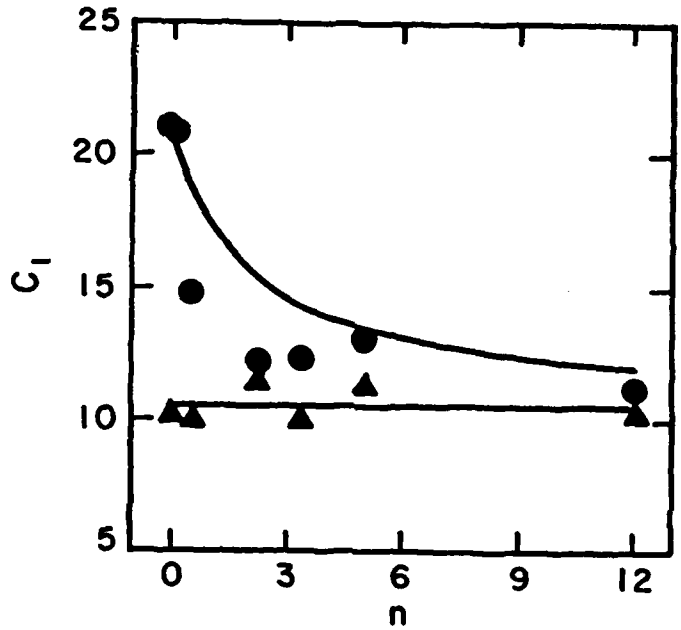

7. WLF constant C_1 versus mer index n of DGEBA. triangles - σ, circles - f_{max}

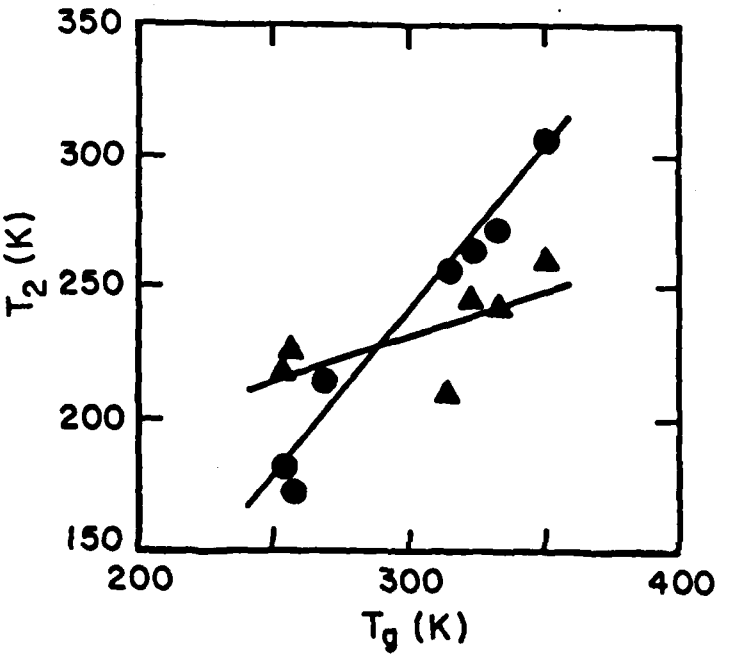

8. Gibbs-DiMarzio second order transition temperature, T_2, versus glass transition temperature of DGEBA.
triangles - σ, circles - f_{max}

DISTRIBUTION LIST

Dr. J. M. Augl
Naval Surface Weapon Center
White Oak, MD 20910

Prof. F. J. Boerio
Dept of Materials Science
U. of Cincinnati
Cincinnati, OH 45221

Prof. H. F. Brinson
Center for Adhesion Science
VPI&SU
Blacksburg, VA 24061

Dr. M. Broadhurst
National Bureau of Standards
Gaithersburg, MD 20899

Dr. Charles Browning
AFWAL/ML
WPAFB, OH 45433

Dr. Stan Brown
NADC
Warmenster, PA

Defense Technical Information Center
Cameron Station
Alexandria, VA 22314
(12 Copies)

Dr. Dawn Dominguez
Naval Research Laboratory
Washington, D.C. 20375

Dr. L. T. Drzal
AFWAL/MLBM
WPAFB, OH 45433

Prof. D. W. Dwight
Center for Adhesion Science
VPI&SU
Blacksburg, VA 24061

Dr. R. B. Fox
NRL Code 6120
Washington, D.C. 20375
Akron, OH 44304

Dr. Alan Gent
Institute of Polymer Science
University of Akron
Akron, OH 44304

Prof. Brian Hornbeck
U. S. Army R&D Center
STRBE-NBC
Ft. Belvoir, VA 22060

Dr. Don Hunston
Polymer Division
National Bureau of Standards
Gaithersburg, MD 20899

Prof. Wolfgang Knauss
Graduate Aeronautical Labs
California Technical
Pasadena, CA 91125

Dr. W. B. Moniz
Naval Research Laboratory
NODE 6120
Washington, DC 20375

Dr. L. H. Peebles, Jr.
Office of Naval Research
Code 431
800 N. Quincy St.
Arlington, VA 22217-5000
(2 copies)

Dr. R. R. Reeber
ARO
PO Box 12211
Research Triangle Park, NC 27709

Dr. Z. N. Sanjana
Westinghouse R&D Center
Pittsburgh, PA 15235

Prof. S. D. Senturia
MIT
Rm 13-3010
Canbridge, MA 02139

Dr. Robert Timme
NRL/USRD
Orlando, FL 32806

Dr. Ting
NRL/USRD
Orlando, FL 32806

Dr. Ron Trabocco
Code 60631
NADC
Warminster, PA

DISTRIBUTION LIST

Dr. J. D. Venables
Martin Marrietta Labs
Dept of Chemical Engineering
Princeton University, Wentworth
Princeton, N.J. 08540

Prof. T. C. Ward
Center for Adhesion Science
VPI&SU
Blacksburg, VA 24061

Dr. S. Wentworth
AMXMR-OP AMMRC
Watertown, MA 02172

Prof. J. P. Wightman
Center for Adhesion Science
VPI&SU
Blacksburg, VA 24061

Dr. Henry Wohltjen
Naval Research Laboratory
Code 6100
Washington, D.C. 20375

Dr. K. J. Wynne
Office of Naval Research
Code 413
800 N. Quincy St.
Arlington, VA 22217-5000